Marie Skłodowska-Curie (MSCA) – Innovative Training Networks (ITN)

H2020-MSCA-ITN European Training Networks

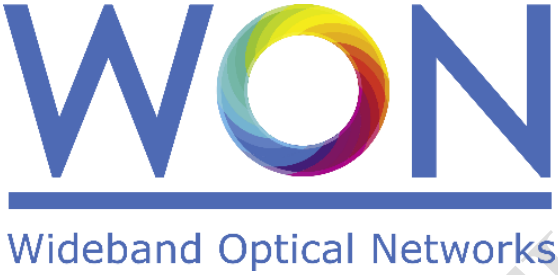

Wideband Optical Networks [WON]

Grant agreement ID: 814276

WP3 – In-line component design

Deliverable D3.4 Evaluation and optimisation of the wideband amplifiers in coherent transmission systems

This project has received funding from the European Union's Horizon 2020 research and innovation programme under the Marie Skłodowska-Curie grant agreement 814276.

Document Details

Work Package	WP3- In-line component design
Deliverable number	D3.4
Deliverable Title	Evaluation and optimisation of the wideband amplifiers in coherent transmission systems
Lead Beneficiary:	Aston University
Deliverable due date:	21 December 2021
Actual delivery date:	29 November 2022
Dissemination level:	Public

Project Details

Project Acronym	WON
Project Title	Wideband Optical Networks
Call Identifier	H2020-MSCA-2018 Innovative Training Networks
Coordinated by	Aston University, UK
Start of the Project	1 January 2019
Project Duration	48 months
WON website:	https://won.astonphotonics.uk/
CORDIS Link	https://cordis.europa.eu/project/rcn/218205/en

WON Consortium and Acronyms

Consortium member	**Legal Entity Short Name**
Aston University	Aston
Danmarks Tekniske Universitet	DTU
VPIphotonics GmbH	VPI
Infinera Portugal	INF PT
Fraunhofer HHI	HHI
Politecnico di Torino	POLITO
Technische Universiteit Eidhoven	TUE
Universiteit Gent	UG
Keysight Technologies	Keysight
Finisar Germany GmnH	Finisar
Orange SA	Orange
Technische Universitaet Berlin	TUB
Instituto Superior Tecnico, University of Lisboa	IST

CONTENTS

ABBREVIATIONS

BDFA: Bismuth-doped fibre amplifier
CAPEX: Capital expenditure
CRF: Corning Raman fibre
CUT: Channel under test
DRA: Discrete Raman amplifiers
EDFA: Erbium-doped fibre amplifier
ISRS: Inter-channel stimulated Raman scattering
MBT: Multiband transmission
NF: Noise figure
OSA: Optical spectrum analyzer
OSNR: Optical signal-to-noise ratio
PCE: Power conversion efficiency
SMF: Single mode fibre
SOA: Semiconductor optical amplifier
TDFA: Thulium-doped amplifier
UWB: Ultra-wideband
ISRS: Inter-channel stimulated Raman scattering

LIST OF FIGURES

EXECUTIVE SUMMARY

The present scientific deliverable is a part of the Work Package 3 “Inline component design” of ETN project WON “Wideband Optical Network”, funded under the Horizon 2020 Marie Sklodowska-Curie scheme Grant Agreement 814276
This document provides an overview of Raman and Bismuth doped fibre amplifiers, validated over a coherent transmission system. For the Raman amplifier, the characterized amplifier presented in D3.3 was validated over a coherent transmission system using a 30 GBaud PM-16QAM signal coupled together with 146x100 GHz ASE channels covering the E-, S-, C- and L-band of the optical window. Our experiment results show a performance penalty (Q^2 penalty) of ~4 dB for the E- and S-band, whereas for C- and L-band this was ~2dB. In addition, we report a first-time ultra-wideband transmission through 70-km long fibre enabled by a hybrid amplifier based on bismuth-doped fibre and discrete Raman amplification. The experiment features 195-nm 30 GBaud PM-16-QAM signals amplified with 15 dB gain and 6 dB NF.

1. Introduction

As explained previously in D3.3 multiband transmission (MBT) is an interesting approach to address the demand for data that is exponentially rising with each year [1]. The development of an MBT architecture requires system upgrade at both node and operator level as the existing infrastructure is designed to support only the C-band of the optical window [2]. Analysis has shown the performance of MBT with existing C-band systems [3] and numerous research reports have experimentally demonstrated coherent MBT with these existing technologies, exhibiting the potential of MBT for next-generation optical communication. In terms of high throughput data using coherent MBT a net throughput of 256.4 Tb/s estimated from GMI and 244.3 Tb/s from LDPC decoding was achieved by combining distributed Raman with TDFA and EDFA for an S-, C- and L-system [4]. S-, C- and L-band transmission was also performed with doped fibre amplifiers, TDFAs, and EDFAs, in the inline stage where a net throughput of 178.08 Tb/s was achieved using SNR-tailored geometric shaping in [5]. In addition, a net throughput of 150.3 Tb/s was also reported by Hamaoka et al where launch power optimization was demonstrated to minimize inter-channel stimulated Raman scattering (ISRS) [6].
In addition to the above-mentioned data rates with high cardinality, coherent transmission over a bandwidth of 157 nm covering the S-, C-, and L-band was reported in [4], [7]. In this work, we demonstrated coherent transmission over a bandwidth of 195 nm using all discrete Raman and hybrid Raman/BDFA covering the E-, S-, C-, and L-band of the optical window [8]. Our first test case included a multistage Raman amplifier in the inline stage, where coherent transmission using 30 GBaud PM-16QAM was performed over a transmission distance of 70 km using standard C-band components. We report an error-free transmission within an assumed HD-FEC threshold of 8.5 dB over a bandwidth of 195 nm extending from 1410-1605 nm. Our experimental results show a maximum Q^2 penalty of ~4 dB for E- and S-band and ~2 dB for C- and L-band. To the best of our knowledge, this is the highest bandwidth coherent transmission validated using DRA. In the next step, the E-band Raman was replaced with an in-house BDFA, and for the S,-C- and L-band a dual stage Raman amplifier was used for inline amplification. This hybrid architecture of BDFA/ Raman was validated over a coherent transmission system and similar to our previous test case, we report an error free transmission over a transmission bandwidth of 195 nm within an assumed HD-FEC threshold of 8.5 dB.

Moreover, we present a first-time implementation of an ultra-wideband amplifier based on a combination of a discrete Raman amplifier (DRA) for the S-, C-, and L-bands and a BDFA for the E-band. The MB amplifier performance was characterized in terms of a gain average of 15 dB, and noise figure (NF) - 6 dB. Moreover, a 70 km, 195 nm transmission of dual-polarization (DP) 30 GBaud 16-QAM signals is realized using this MB amplifier. Our experimental results show a low Q^2 factor penalty (less than 3.5 dB) for all the transmission bands. Moreover, two further BDFAs were used in the booster and receive stages to enable E-band transmission, showing comparable performance with commercially available amplifiers used for the same function in S-, C-, and L-bands.

2. Coherent transmission with the multistage discrete Raman amplifier

2.1 Experimental setup

The multistage DRA characterized in D3.3 was validated over a coherent transmission system. The schematic of the multistage DRA and the characterization results of the amplifier (gain/NF, output OSNR) is shown below in Figure 1 (a-c). A detailed explanation of the amplifier characteristics is presented in D3.3.

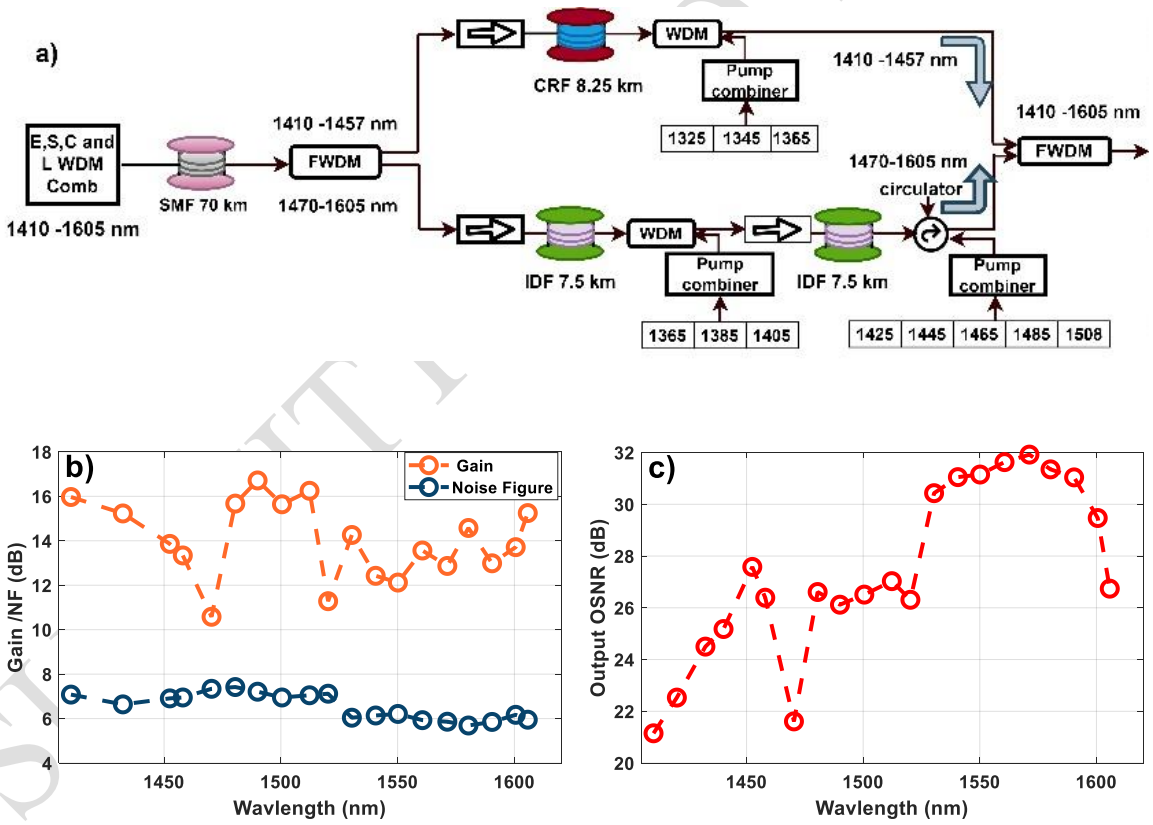

Figure 1: Multistage discrete Raman amplifier a) Schematic b) Gain/ Noise figure and c) amplifier output OSNR

To evaluate the performance penalty of our proposed amplifier, the coherent transmission was performed over a 70 km standard SMF with the multistage DRA in the inline stage, as illustrated in Figure 2(a). In the transmitter (Tx) section, a 30 GBaud DP-16QAM signal was generated using a 120 GSa/s digital-to-analog converter (DAC) and a standard C-band $LiNBO_3$ DP-IQ modulator. Two external cavity laser sources extending from (1410 -1480 nm) and (1480- 1620 nm) were used in the

transmitter (Tx) section to emulate the WDM carrier from (1410-1605 nm). The modulated signal was then amplified using booster amplifiers for different channels, this includes C- and L-band EDFAs for channels in the wavelength range of 1530-1605 nm, TDFA for S-band (1470-1520 nm) and an in-house BDFA for E-band (1410-1460 nm), whose detailed is presented in D3.3. The modulated signal was equalized to the same level as the ASE channels using a variable optical attenuator (VOA) and then coupled with the WDM grid comprising 143x100 GHz channelized ASE signals extending from 1470-1605 nm and three continuous wave laser sources at 1411,1431 and 1451 nm using a 90/10 coupler. In the SMF input section, the total power was ~19.6 dBm with an approximate power per channel of -2 dB. The WDM signals were then passed through a standard SMF of 70 km where the total power loss was ~14.8 dB for the entire grid. These attenuated signals were then amplified using the proposed multistage DRA as an inline amplifier to compensate for the SMF power loss. Even though the multistage DRA can amplify signals up to 1620 nm (210 m), we were restricted to a bandwidth of 195 nm due to the bandwidth limitation of the booster and pre-amp L-EDFA. After the inline amplification, the signals were then passed through a 99/1 tap whose 1% was used to capture the spectrum and measure the amplifier output OSNR, and whose remaining 99% power was transferred to the receiver (Rx) chain for performance penalty analysis using a standard coherent detection procedure.

In the receiver (Rx) section the modulated signal was filtered using a wideband optical band-pass filter (OBPF) having an average insertion loss of 5 dB. After the separation stage, the modulated signal was passed to the corresponding Rx amplifiers (BDFA, TDFA, C- EDFA, and L- EDFA) to provide the necessary output power for optimal operation of the coherent Rx. For the E-band signals, a VOA was added to the output of the BDFA to control the output power. This was primarily due to the absence of a commercial BDFA that can be operated in a constant output power mode. The modulated signal was then mixed with an external local oscillator for balance detection. The signals were received using a standard coherent receiver where corresponding traces were captured with four photodetectors and a frontend 80 GSa/s (36 GHz analog bandwidth) real-time oscilloscope. The detection procedure was followed by standard offline DSP for data recovery on the captured traces. The recorded symbols together with the transmitted symbols were then used to derive the Q^2 factor from the hard decision bit error rate (BER) [9][10].

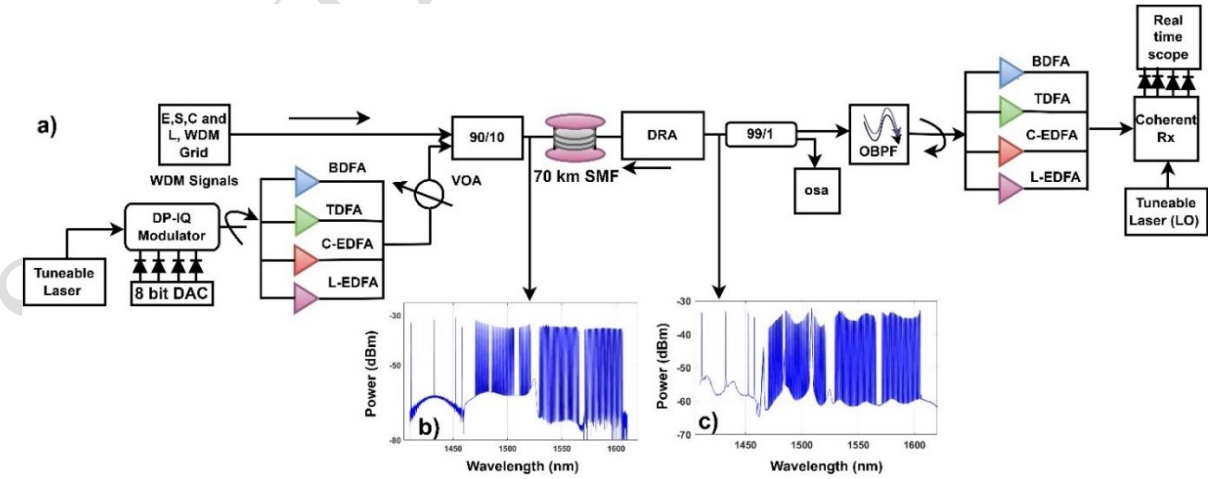

Figure 2: Coherent transmission of E-, S-, C- and L-band WDM signals a) schematic of setup b) input spectrum b) output spectrum

2.2 Results and discussion

Figures 2(b-c) show the input spectrum to the SMF and output spectrum after DRA. As one can observe, guard bands of +/- 2nm and +/- 3 nm were kept around the 1485 and 1508 nm pumps to prevent the overlapping of the channelized ASE and the pump. The detained analysis of the method is explained in [11]. Figure 3 shows the constellation diagram of back-to-back (B2B) system performance and the transmission performance after 70 km transmission of 1430, 1500, 1550 and 1605 nm signals. The constellation of the 1550 nm signal after post-equalization has the best B2B performance with a minimum noise level, whereas the noise level is maximum for the 1430 nm signals. This difference in the B2B performance for the wavelengths in different bands indicates the system limitations when operated in different windows of optical communication. Similarly, after 70 km, the best constellation was observed for the 1550 nm signal with minimum noise, whereas noisier constellations were seen for the other bands with a maximum for the 1430 nm signal. The higher noise in the B2B constellations for 1430, 1500, and 1605 nm signals in comparison to 1550 nm signals, can be attributed to the performance limitation due to the combined effect of the amplifiers (booster, Rx amplifier) and other transceiver components when operated in the E-, S- and L-band, with the use of standard C-band components. As for the constellation after 70 km the higher noise levels in the E- and S-bands can be attributed due to the lower received OSNR, and high NF of the amplifiers.

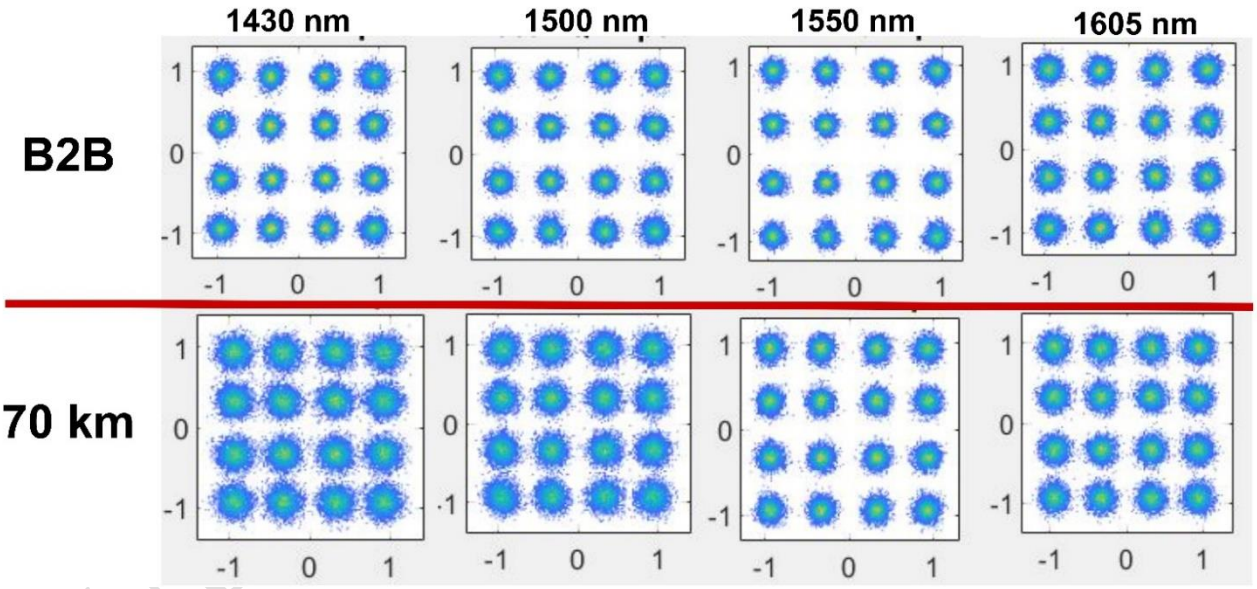

Figure 3: Constellation diagram for B2B and 70km transmission for 1430, 1500, 1550, and 1605 nm channels.

The performance of the UWB transmission with the multistage stage DRA in the inline stage can be seen below in Figure 4(a-c). Our transmission results (Q^2 Factor) show a degrading B2B performance (blue line with circle marker) for E-band (1410-1457 nm) in comparison to C- and L-band (1470-1605 nm) with a 2.5 dB roll-off. This degradation is primarily due to the use of the standard C-band transceiver components in particular. The major performance degradation due to the component limitation comes from the I/Q imbalance of the transmitter and the polarization imbalance of the optical hybrid in the receiver stage [3]. In addition, the passive components also has higher insertion losses which result in the driving of the amplifier at maximum current to compensate for the additional losses.

These effects eventually degrade the received OSNR for the lower wavelength signals. For signals in the range of 1470-1520 nm, a variation of ~ 2 dB was observed with the lowest value being 16 dB for the 1470 nm signal. This degradation in performance specifically towards the lower wavelength in S-band is due to the high NF of the Tx/Rx TDFA. A steady performance of ~ 18 dB (B2B) can be seen in the C-band (1530-1570 nm) which then eventually degrades down to 16.5 dB at 1605 nm in the L-band.

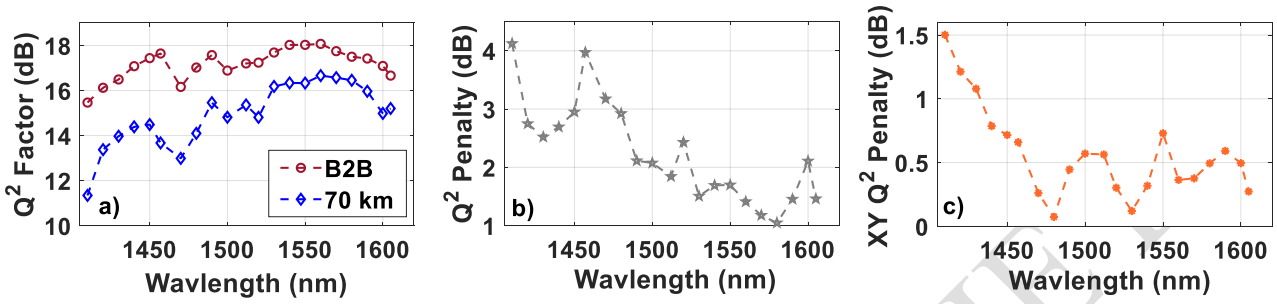

Figure 4: PM-16 QAM 30 GBaud transmission result; wavelength vs a) Q^2 Factor b) Q^2 Penalty b) XY Q^2 Penalty

The Q^2 factor after 70 km transmission illustrated in Figure 4a (blue line with diamond marker) follows the same trend as the B2B curve for the entire bandwidth. The Q^2 penalty shown in Figure 4b is the difference in the Q^2 factor between B2B and 70 km transmission. Signals in the range of 1530-1620 (E- and S-band) nm show a lower Q^2 penalty with its maximum penalty being ~2 dB at nearly 1600 nm. However, for the signals from 1410-1520 nm (E- and S-band), a higher penalty was observed with a maximum value of ~4 dB for 1410 and 1470 nm signals. The average Q^2 penalty in E- and S-band was around 3 dB whereas, for C- and L-band this value was ~1.5 dB. The trend in the Q^2 penalty can be largely correlated to the NF and output OSNR of the spectral bands shown in Figure 1 (b-c), where the maximum NF of the DRA was in the region of E- and S-band with an output OSNR <28 dB. Similarly, in the C- and L bands the NF was lower with an output OSNR of ~30 dB across the entire bandwidth. The C- and L-band signals also benefit from ISRS power transfer from the S-band channels in the DRA stage1 of the dual-stage configuration, improving the overall performance and subsequently degrading the performance of the E- and S-band signals.

As explained above, UWB transmission undergoes performance degradation due to I/Q and polarization imbalance, with the use of a standard C-band modulator and optical hybrid for E-, S-, and L-band. To investigate the effects of polarization imbalance due to the standard optical hybrid we measured the XY Q^2 penalty (Figure 4(c)). This parameter relates to the difference in the Q^2 factor for X and Y polarization. As can be seen from Figure 4(c), the penalty for signals > 1480 nm was <0.6 dB whereas, on the other hand, a linear increment in the penalty was observed for signals < 1470 nm with the maximum value being 1.5 dB for 1410 nm signals. In addition to the high NF and low OSNR of the E-band signals, the large polarization imbalance in the optical hybrid particularly for E-band signals is a major factor in the degradation of the Q^2 factor and Q^2 penalty. The overall performance of E- and S-band can be improved by both the optimized design of the DRA and the replacement of C-band components with low-loss optical components specifically targeting these bands.

3. Coherent transmission with the multi-band amplifier enabled by bismuth-doped fibre and discrete Raman amplification

The schematic of the ESCL-band amplifier is presented in Fig. 5(a). It comprises two separate optical paths, with a BDFA operating in the E-band and a dual-stage DRA operating in the S-, C-, and L-bands. These bands are separated by a filter WDM (FWDM), with transmission and reflection bands of 1410-1457 nm and 1470-1620 nm. After band-splitting, the E-band signal follows the upper path in Fig. 5(a) passing via an isolator to a 300 m long Bi-doped fibre that is bi-directionally pumped via a pair of WDM couplers by two pump diodes at 1260 nm (forward) and 1310 nm (backward). Additionally, two isolators are used to ensure unidirectional propagation of the signal. The Bi-doped fibre used in this paper is the one reported in [12]. The SCL-band signal follows the lower path in Fig. 5(a) where the first stage of the amplifier targets S-band amplification, and consists of an isolator, 7.5 km-long inverse dispersion fibre (IDF), WDM, a pump combiner and three pump diodes at 1365 nm, 1385 nm, and 1405 nm. The second stage amplifies the C- and L-bands and consists of the same set of components with the exception of pump combiner and pump laser diodes at 1425 nm, 1445 nm, 1464 nm, 1485 nm, and 1508 nm. Finally, both amplified signals are combined with 1410-1457nm/1470-1620nm FWDM.

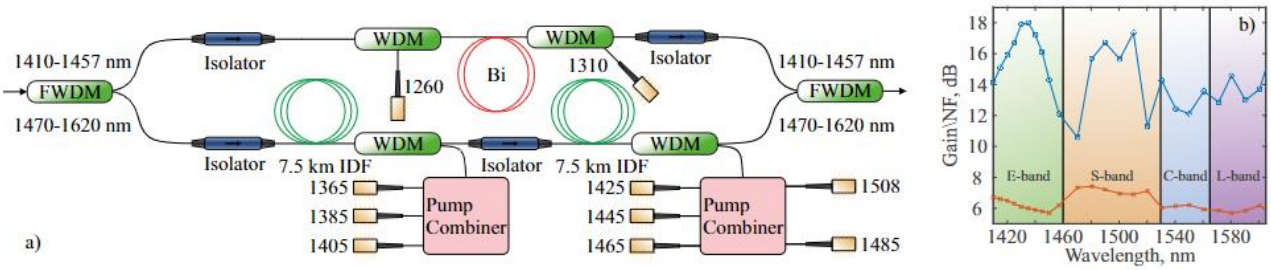

Figure 5: Experimental setup E-,S-,C-,L-band amplifier enabled by active Bi-doped fibre and discrete Rama amplification.

The measured gain and noise figure (NF) of the amplifier are presented in Fig. 5(b), showing a maximum gain of 18 dB and minimum NF of 5.9 dB. The E-band BDFA was pumped at only 200 mW to enable matching gain with the DRA. The reduced gain at 1460 nm is explained by the lower efficiency of the BDFA in this region at this relatively low pump power level. The minimum of the NF is at 1450 nm which corresponds well with the behaviour reported previously [11]. The DRA has increased gain in the S-band except in the vicinity of 1470 nm and 1520 nm due to high attenuation values, inter stimulated Raman scattering (ISRS) power transfer to the C and L band signals, and limitations of the pump. The NF was found to be lowest in the C-band with a minimum value 5.9 dB NF. The DRA has flat gain (with variations less than 3dB) from 1520 nm to 1605 nm with average gain of 13 dB covering whole C and L bands. The setup of the data transmission experiment is presented in Fig. 6(a). The E-, S-, C-, L-band WDM grid consists of 143x100 GHz ASE- emulated channels in the S-, C-, and L-bands, plus three E-band laser diodes at wavelengths of 1411 nm, 1432 nm, and 1451 nm (Fig. 6(b,c,d)). The S-band channels (1470-1520 nm) are generated using a supercontinuum source and a commercial wavelength selective switch (WSS) for channel spacing and flattening followed by a thulium doped fibre amplifier (TDFA). There are also two guard bands of 4 nm and 6 nm around each of the longest wavelength pumps at 1485 nm and 1508 nm, respectively. The S-band channels are combined together with a flat channelised C and L-band ASE noise

extending out to 1608 nm, generated using C and L-band EDFAs and two WSSs for equalization and flattening. The data carrier signal is generated using different tuneable lasers operating from 1410 to 1605 nm, which are modulated by a dual-polarization IQ modulator (DP IQ Mod) driven by a digital-to-analog converter (DAC) to achieve 30 GBaud 16 QAM signals. The signal after the modulator is amplified by a booster amplifier (in-house BDFA for E-band, commercial TDFA for S-band, and commercial EDFAs for C- and L-bands). For power equalization of the data channel with WDM grid, a variable optical attenuator (VOA) is used ahead of a 90/10 coupler. As the WDM grid is dense in the S-, C-, and L-bands, the WDM channel corresponding to the data carrier signal is turned off by a WSS to avoid channel overlap. In the case of back-to-back (B2B) transmission, the signal is then directed to an optical bandpass filter (OBPF), where the data carrier is filtered. When the transmission is performed, the signal is directed into a 70 km-long SMF-28 fibre and then amplified by the developed hybrid MB amplifier. In both cases, after the data carrier is filtered by the OBPF, it is amplified by an appropriate receive amplifier, similarly to the booster. The input power to the coherent receiver is controlled by another VOA, and a set of external tuneable lasers operating from 1410-1605 nm is used as a local oscillator for the coherent detection system. Channel reception is completed by a standard set of 80 GSa/s analog-to-digital converters (ADCs).

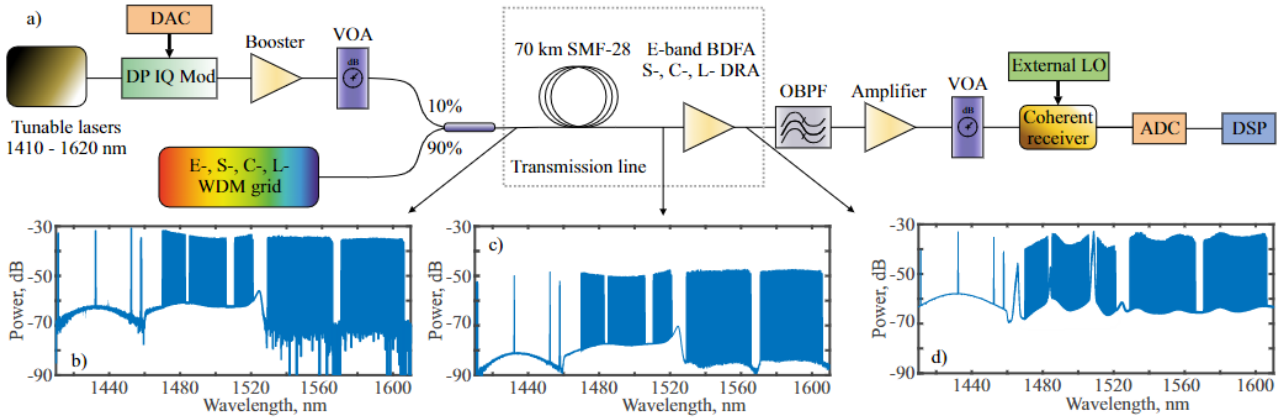

Figure 6: a) Experimental setup of a B2B and transmission experiment; spectra of the WDM grid and E-band data carrier signal at 1457 nm at (b) input to the span, (c) end of the span, (d) after the amplifier.

The recorded results of the transmission experiment are presented in Figure 7. The wavelength dependence of the Q^2 factor of a DP 30 GBaud 16 QAM signal is recorded by tuning the wavelength of the tuneable lasers (signal and local oscillator) across 195-nm bandwidth from 1410 to 1605 nm. The wavelength dependencies of the Q^2 factor (average between X and Y) for B2B and 70 km-long transmission are presented in Fig. 7(a). The Q^2 factor was calculated from the signal-to-noise ratio obtained from the recovered constellations [9]. The transmission performance of the DRA in the L-band features a Q^2 factor penalty no higher than 2.2 dB and the lowest Q^2 factor penalty for the whole DRA of just 1 dB (Fig. 7,b). The C-band shows the best B2B performance achieved in the experiment, enabled by the commercial EDFAs. The DRA has a maximum Q^2 factor penalty of 1.7 dB in this region. The B2B performance in the S-band shows similar performance to the L-band. However, a noticeable decrease of the S-band B2B performance at around 1470 nm is due to the relatively high NF of the TDFA in this region. The performance of the DRA in the S-band has a maximum penalty of

3.3 dB and the minimum of 2 dB. The substantial increase of the Q^2 factor penalty at 1470 nm can be explained by the high NF of the DRA at this wavelength of operation.

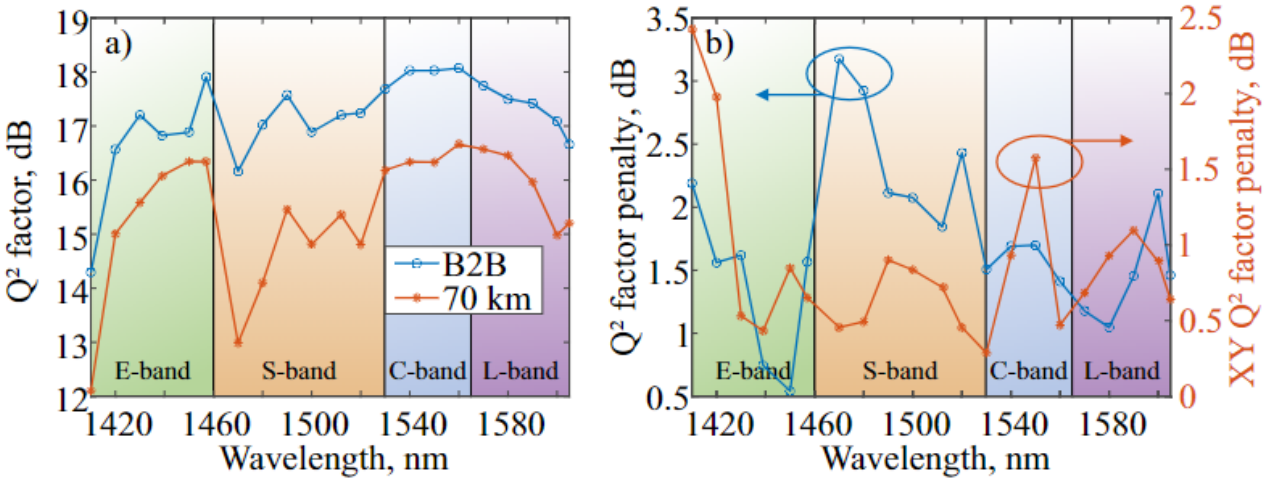

Figure 7: a) Wavelength dependency of the Q^2 factor for B2B case and 70-km long transmission; b) wavelength dependency of Q^2 factor penalty between B2B case and transmission (blue line with circles) and X and Y polarization Q^2 factor imbalance (orange line with stars)

The E-band B2B measurement was enabled by two in-house-made BDFAs that will be reported elsewhere. The general B2B performance level is similar to the L-band case. However, there is a significant decrease of the performance at 1410 nm. This can be explained by substantial limitations of the optical hybrid in terms of polarization balance starting at 1420 nm. The X and Y polarization imbalance penalty is presented in Figure 7(b). There is a significant increase of the X and Y impairment below 1430 nm. The commercial optical hybrid used in this experiment was optimized for operation in the C- and L- optical bands. Despite the limited operation bandwidth, the X-Y impairment is lower than 2.5 dB in the whole region from 1430 to 1605 nm. The E-band transmission features the lowest Q^2 factor penalty of just 0.5 dB. Otherwise, the general performance of the in-line BDFA is similar to C- and L-band DRA. The increase of penalty towards 1410 nm is explained by both rising NF and decreasing gain of the amplifier.

4. Conclusions

In this deliverable, we validated our proposed multistage discrete Raman amplifier over a coherent transmission system covering the E-, S-, C- and L-band of the optical window. WDM transmission was performed with a 30 GBaud PM-16QAM signal coupled with 143x100 GHz ASE channels for S-C, and L-band and 3 continuous wave laser diodes in the E-band. Our experimental results shows error-free transmission over a SMF length of 70 km with a maximum Q^2 penalty of ~ 2 dB for C- , L-band and ~4 dB penalty for E- , S-band signals. To the best of our knowledge this is the highest bandwidth (195 nm) of coherent transmission validated experimentally using a DRA. Based on our experimental results, we can conclude that the Raman amplifier is a potential candidate for signal amplification and can be implemented as an inline amplifier in an MBT systems. Performance of MBT systems using a DRA in the inline stage can be improved by proper optimization of pump powers and wavelengths, along with the development of low loss, high Raman gain fibre. In addition to amplifier

optimization, the overall performance of a MBT system can be further enhanced with the design and development of low loss optical components specifically targeting these bands.

In addition, an ultra-wideband amplifier was developed and demonstrated with maximum gain of 18 dB and minimal NF of 5.9 dB. The amplifier was enabled by Bi-doped fibre in the E-band and discrete Raman amplification in S-,C-,L-bands. A transmission experiment of 195 nm dual polarisation 30 GBaud 16 QAM signal through 70 km was conducted to study further the performance of the developed amplifier. The overall performance of the amplifier was investigated and the average Q^2 factor penalty is around 1.7 dB through investigated bands. The minimal Q^2 factor penalty of just 0.5 dB at 1450 nm was achieved by amplification in Bi-doped fibre. We believe that our results show a great potential of using Bi-doped fibre amplifier in combination with discrete Raman amplifier for ultra-wideband transmission in E-, S-, C-and L-bands.

5. REFERENCES

[1] P. J. Winzer, D. T. Neilson, and A. R. Chraplyvy, “Fiber-optic transmission and networking: the previous 20 and the next 20 years [Invited],” *Opt. Express*, vol. 26, no. 18, p. 24190, 2018, doi: 10.1364/oe.26.024190.

[2] A. Ferrari *et al.*, “Assessment on the Achievable Throughput of Multi-Band ITU-T G.652.D Fiber Transmission Systems,” *J. Light. Technol.*, vol. 38, no. 16, pp. 4279–4291, 2020, doi: 10.1109/JLT.2020.2989620.

[3] R. Emmerich *et al.*, “Enabling S-C-L-band systems with standard C-band modulator and coherent receiver using nonlinear predistortion,” *J. Light. Technol.*, vol. 40, no. 5, pp. 1360–1368, 2021, doi: 10.1364/ofc.2021.f4d.7.

[4] B. J. Puttnam, R. S. Luís, G. Rademacher, M. Mendez-Astudillio, Y. Awaji, and H. Furukawa, “S-, C- and L-band transmission over a 157 nm bandwidth using doped fiber and distributed Raman amplification,” *Opt. Express*, vol. 30, no. 6, p. 10011, 2022, doi: 10.1364/oe.448837.

[5] L. Galdino *et al.*, “Optical Fibre Capacity Optimisation via Continuous Bandwidth Amplification and Geometric Shaping,” *IEEE Photonics Technol. Lett.*, vol. 32, no. 17, pp. 1021–1024, 2020, doi: 10.1109/LPT.2020.3007591.

[6] F. Hamaoka *et al.*, “Ultra-wideband WDM transmission in S-C- A nd L-bands using signal power optimization scheme,” *J. Light. Technol.*, vol. 37, no. 8, pp. 1764–1771, 2019, doi: 10.1109/JLT.2019.2894827.

[7] M. Asif Iqbal, L. Krzczanowicz, I. Phillips, P. Harper, and W. Forysiak, “150nm SCL-band transmission through 70km SMF using ultra-wideband dual-stage discrete raman amplifier,” in *Optical Fiber Communications Conference and Exhibition (OFC)*, 2020, no. c, pp. 1–3. doi: 10.1364/OFC-2020-W3E.4.

[8] P. Hazarika *et al.*, “E-, S-, C- and L-band coherent transmission with a multistage discrete Raman amplifier PRATIM,” *Opt. Express*, vol. 30, no. 24, pp. 43118–43126, 2022, doi: 10.1364/ofc.2022.tu3e.2.

[9] P. Skvortcov *et al.*, “Nonlinearity Tolerant LUT-Based Probabilistic Shaping for Extended-Reach Single-Span Links,” *IEEE Photonics Technol. Lett.*, vol. 32, no. 16, pp. 967–970, 2020, doi: 10.1109/LPT.2020.3006737.

[10] A. D. Ellis, M. E. McCarthy, M. A. Z. Al Khateeb, M. Sorokina, and N. J. Doran, “Performance limits in optical communications due to fiber nonlinearity,” *Adv. Opt. Photonics*, vol. 9, no. 3, p. 429, 2017, doi: 10.1364/aop.9.000429.

[11] M. A. Iqbal *et al.*, “Impact of pump-signal overlap in S+C+L band discrete Raman amplifiers,” *Opt. Express*, vol. 28, no. 12, p. 18440, 2020, doi: 10.1364/oe.392258.

[12] A. Donodin *et al.*, “Bismuth doped fibre amplifier operating in E- and S- optical bands,” *Opt. Mater. Express*, vol. 11, no. 1, p. 127, 2021, doi: 10.1364/ome.411466.